Proceeding of the 2004 American Control Conference
Boston, Massachusetts June 30 - July 2, 2004

A Trajectory Tracking of Legged Robot Using Decentralized Control with Robustness Designs

Chih-Lyang Hwang (clhwang@ttu.edu.tw) and Chung-Wen Chang
Department of Mechanical Engineering, Tatung University, Taipei, 10451 Taiwan, R.O.C.

Abstract -- In this paper, a microprocessor-based decentralized sliding-mode tracking control was applied to a legged robot with two-degree-of-freedom. Under no external load, a linear discrete-time dynamic model for every link was individually achieved by the recursive least-squares parameter estimation. An output disturbance caused by the interaction and modeling error deteriorated the system performance. In this situation, a minimax optimization of the weighted sensitivity between the output disturbance and switching surface was obtained to attenuate the effect of the output disturbance. Moreover, a suitable selection of the weighted function could reject the output disturbance of known mode. For further improving the system performance, a switching control was designed. Finally, the experiments for the legged robot with (or without) payload was arranged to evaluate the usefulness of the proposed method.

I. INTRODUCTION

As one knows, the dynamics of a legged robot is coupled and complex [1]. Hence, a centralized control is neither economically feasible nor even necessary [2]. Because the decentralized control scheme avoids difficulties in complexity of design, debugging, data gathering, and storage requirements, it is more preferable for the legged robot than a centralized control. In this situation, a decentralized control is considered. Under no external load, a linear discrete-time dynamic model for every link is individually achieved by the recursive least-squares parameter estimation, e.g., [3]. Due to the coupled characteristics of the legged robot and the existence of modeling error, an output disturbance depreciates the system performance or results in the system instability. Therefore, how to design an effective and simple controller for a legged robot is of paramount importance.

It is well-known that sliding-mode control contains several advantages, e.g., fast response, less sensitive to uncertainty, and easy implementation [4]. A dead-beat to switching surface is first obtained to track the desired trajectory [5]. A minimax optimization of the weighted sensitivity between the output disturbance and switching surface is then obtained to reduce the effect of the output disturbance. In addition, a suitable selection of the weighted function can reject the output disturbance of known mode. It is the so-called “optimal and rejected robustness”. Although the effect of the output disturbance is attenuated or rejected, a better performance can be improved by a switching control based on the Lyapunov redesign. This is another aspect of the paper, which is called as “improved robustness”.

The DSP-chip of TMS320F240 is employed to realize the proposed control. The TMS320F240 has many good features that make it a good candidate to implement the proposed control. Finally, the experiments of the legged robot with (or without) payload for different controllers are given to confirm the usefulness of the proposed control scheme.

II. SYSTEM DESCRIPTION AND PROBLEM FORMULATION

2.1 Experimental Setup

Fig. 1 shows the experimental setup of the legged robotic system. The details of Fig. 1 are described in section 4.1. Before modeling the legged robot, a proportional control $K_p = diag\{k_p^1 \quad k_p^2\}, k_p^i = 27, i = 1,2,$ is applied to improve the dynamics of the legdxged robot (see Fig. 2). Then two linear discrete-time models for the modified legged robot are achieved in the next section.

2.2 Modeling

For brevity, the mathematical notation of this paper is the same as our previous paper [6]. The upper script *i* of a variable denotes the *ith* subsystem of the legged robot. Assume that the legged robot is described as follows:

$$Y_p(k) = F\big(Y_p(k-1),\ldots,Y_p(k-n_y),U(k-1),\ldots,U(k-n_u)\big) \quad (1)$$

where $Y_p(k) = \left[y_p^1(k) \quad y_p^2(k)\right]^T, U(k) = \left[u^1(k) \quad u^2(k)\right]^T$, and $F(\cdot)$ denotes an unknown function of the legged robot.

The random signal with maximum amplitude 0.3 *volt* is employed to drive each motor of the legged robot at one time. Then the input and output pairs of data $\{u^i(k), y_p^i(k)\}$ are attained. These input/output pairs are fed into the following least-squares parameter estimation algorithm:

$$\begin{aligned}
&\hat{\theta}^i(k) = \hat{\theta}^i(k-1) + K^i(k-1)\left[y_p^i(k) - \phi^i(k-1)^T\hat{\theta}^i(k-1)\right] \\
&K^i(k-1) = P^i(k-1)\phi^i(k-1)\left[\gamma^i + \phi^i(k-1)^i P^i(k-1)\phi^i(k-1)\right]^{-1} \\
&P^i(k) = \left[I - K^i(k-1)\phi^i(k-1)^T\right]P^i(k-1)/\gamma^i \\
&\phi^i(k-1) = \left[-y_p^i(k-1)\ldots - y_p^i(k-n^i)\, u^i(k-1)..u^i(k-m)\right]^T
\end{aligned} \quad (2)$$

where $1^- \le \gamma^i \le 1,$ the initial value of $P^i(0) = \alpha^i I$, α^i is large enough, the system degrees n^i, m^i are chosen based on the prior knowledge of the system [3]. After the model verification, an appropriate learned model for the robot leg is expressed as follows:

$$y_p^i(k) = q^{-d^i} B^i(q^{-1})u^i(k)/A^i(q^{-1}), \quad i = 1,2 \quad (3)$$

where $A^i(q^{-1}) = 1 + a_1^i q^{-1} + a_2^i q^{-2}, B^i(q^{-1}) = b_0^i + b_1^i q^{-1}$, $d^i = 1$

$a_1^1 = -1.059715, a_2^1 = 0.119491, b_0^1 = -0.079589, b_1^1 = 0.139365$

$a_1^2 = -0.903230, a_2^2 = -0.016889, b_0^2 = -0.164052, b_1^2 = 0.243933.$

0-7803-8335-4/04/$17.00 ©2004 AACC

These two subsystems are stable, in non-minimum phase, and coprime. Because the other sinusoidal responses are similar with Fig. 3, only one sinusoidal response is shown. It indicates that the modeling is acceptable.

2.3 Problem Statement

Based on the approximation theory,

$$Y_p(k) = F\big(Y_p(k-1),...,Y_p(k-n_y),U(k-1),...,U(k-n_u)\big)$$
$$= \begin{pmatrix} q^{-d^1} B^1(q^{-1})u^1(k)\big/A^1(q^{-1}) + d_o^1(k) \\ q^{-d^2} B^2(q^{-1})u^2(k)\big/A^2(q^{-1}) + d_o^2(k) \end{pmatrix} \tag{4a}$$

where the output disturbance is relatively bounded:

$$\left|d_o^i(k)\right| \le \alpha_0^i + \alpha_1^i\left|u^1(k-1)\right| + \alpha_2^i\left|u^2(k-1)\right|, i=1,2 \tag{4b}$$

where α_0^i, α_1^i and $\alpha_2^i, i=1,2$ are bounded. The reference input to be tracked is assigned as follows:

$$r^i(k) = G_r^i(q^{-1})\delta(k)\big/F_r^i(q^{-1}) \tag{5}$$

where $G_r^i(q^{-1})$ and $F_r^i(q^{-1})$ are coprime.

The proposed control is assumed as the following form:

$$R^i(q^{-1})u^i(k) = -S^i(q^{-1})y^i(k) + T^i(q^{-1})r^i(k) + u_{sw}^i(k) \tag{6a}$$
$$y^i(k) = y_p^i(k) + d_o^i(k) \tag{6b}$$

where $d_o^i(k)$ is caused by the modeling error or external load, $y^i(k)$ denotes the real position of the legged robot, the polynomials $R^i(q^{-1}), S^i(q^{-1})$ and $T^i(q^{-1})$ are found to obtain an equivalent control, and $u_{sw}^i(k)$ represents a switching control to improve the system performance.

For safety, the real control inputs (i.e., $u_r^i, i=1,2$) are limited to 8.5 *volt*. Define the following switching surface:

$$\sigma^i(k) = C^i(q^{-1})e^i(k) \tag{7}$$

where $e^i(k) = r^i(k) - y^i(k)$ and $C^i(q^{-1})$ is a stable monic polynomial with degree n_c^i. Then the response of $\sigma^i(k)$ from the inputs $r^i(k), d_o^i(k), u_{sw}^i(k)$ is achieved from (4), (6) and (7); i.e.,

$$\sigma^i(k) = P^i(q^{-1})r^i(k) - V^i(q^{-1})d_o^i(k) - Z^i(q^{-1})u_{sw}^i(k) \tag{8a}$$

where

$$P^i(q^{-1}) = C^i(q^{-1})\left[A_c^i(q^{-1}) - q^{-d^i}B^i(q^{-1})T^i(q^{-1})\right]\big/A_c^i(q^{-1}) \tag{8b}$$
$$V^i(q^{-1}) = C^i(q^{-1})A^i(q^{-1})R^i(q^{-1})\big/A_c^i(q^{-1}) \tag{8c}$$
$$Z^i(q^{-1}) = q^{-d^i}C^i(q^{-1})B^i(q^{-1})\big/A_c^i(q^{-1}). \tag{8d}$$

The $A_c^i(q^{-1})$ denotes the characteristic polynomial of the closed-loop system:

$$A_c^i(q^{-1}) = A^i(q^{-1})R^i(q^{-1}) + q^{-d^i}B^i(q^{-1})S^i(q^{-1}). \tag{9}$$

The objectives of this paper are described as follows: (i) The equivalent control (i.e., $R^i(q^{-1}), S^i(q^{-1})$ and $T^i(q^{-1})$) is attained according to the following two requirements: (a) For the nominal system (i.e., $d_o^i(k) = u_{sw}^i(k) = 0$), the response of the operating point is dead-beat to the switching surface. (b)The minimization of $\left\|W^i(q^{-1})V^i(q^{-1})\right\|_\infty$, where $W^i(q^{-1})$ denotes a suitable rational function, is applied to partially reject and attenuate the effect of the output disturbance. (ii) Based on the Lyapunov redesign, the switching control (i.e., $u_{sw}^i(k)$) is designed to improve the performance of the legged robot.

III. CONTROLLER DESIGN

There are three subsections for the decentralized control with robustness designs (DCRD).

3.1Dead-Beat to Switching Surface for Nominal Subsystem

The response of switching surface $\sigma^i(k)$ must have the following form [5]:

$$\sigma^i(k) = H^i(q^{-1})\delta(k) \tag{10}$$

where $H^i(q^{-1})$ is a polynomial with the degree which is the same as the number of dead-beat steps. Comparing (8) with $d_o^i(k) = u_{sw}^i(k) = 0$ and (10) yields

$$\frac{T^i(q^{-1})}{A_c^i(q^{-1})} = \frac{G_r^i(q^{-1})C^i(q^{-1}) - F_r^i(q^{-1})H^i(q^{-1})}{q^{-d^i}B^i(q^{-1})G_r^i(q^{-1})C^i(q^{-1})} \tag{11}$$

Because $A_c^i(q^{-1})$ is stable, the denominator of the right hand side of (11) must be stable. Hence, the following facts are obtained

$$H^i(q^{-1}) = L^i(q^{-1})G_{r-}^i(q^{-1}) \tag{12}$$
$$G_{r+}^i(q^{-1})C^i(q^{-1}) - F_r^i(q^{-1})L^i(q^{-1}) = q^{-d^i}B_-^i(q^{-1})M^i(q^{-1}) \tag{13}$$

where $F_r^i(q^{-1})L^i(q^{-1})$ and $q^{-d^i}B_-^i(q^{-1})$ are coprime, the monic polynomial $L^i(q^{-1})$ has the degree $n_l^i = n_{b_-}^i + d^i - 1$, and the polynomial $M^i(q^{-1})$ has the minimum degree. Assume that

$$R(q^{-1}) = \hat{R}(q^{-1})B^+(q^{-1})\,. \tag{14}$$

From (6), (11)-(14), the following equations are attained

$$A^i(q^{-1})\hat{R}^i(q^{-1}) + q^{-d^i}B_-^i(q^{-1})S^i(q^{-1}) = G_{r+}^i(q^{-1})C^i(q^{-1})X^i(q^{-1}) \tag{15}$$
$$T^i(q^{-1}) = M^i(q^{-1})X^i(q^{-1}) \tag{16}$$

where $X^i(q^{-1})$ is a stable polynomial with the degree $n_x^i = n_a^i + n_{b_-}^i + d^i - n_{g_+}^i - n_c^i - 1$. From (11), (14), (15), and (9), the following nominal closed-loop characteristic polynomial is then achieved

$$A_c^i(q^{-1}) = C^i(q^{-1})G_{r+}^i(q^{-1})B_+^i(q^{-1})X^i(q^{-1}). \tag{17}$$

3.2Minimax Optimization of Weighted Sensitivity Function

Based on a prior paper (e.g., [7]), the optimal $\left\|W^i(q^{-1})V^i(q^{-1})\right\|_\infty$ must satisfy the following interpolation constraints:

$$V^i(p_j^i) = 0, j = 1,2,...,n_{a_-}^i \tag{18a}$$
$$1 - V^i(z_j^i)\big/C(z_j^i) = 0, j = 1,2,...,n_{z_j}^i - 1 \tag{18b}$$

where $n_{z_j}^i = n_{b_-}^i + d^i$, $p_j^i (1 \le j \le n_{a_-}^i)$ and $z_j^i (1 \le j \le n_{z_j}^i\text{-}1)$ denote the zeros of $A_-^i(q^{-1})$ and $q^{-d^i}B_-^i(q^{-1})$, respectively.

According to the result of *Lemma 1* in [8] and the constraint (18), the following equation is achieved

$$V^i(q^{-1}) = \rho^i W_d^i(q^{-1})A_-^i(q^{-1})\bar{\Phi}^i(q^{-1})\big/\left[W_n^i(q^{-1})\bar{A}_-^i(q^{-1})\Phi^i(q^{-1})\right] \tag{19}$$

where $W^i(q^{-1}) = W_n^i(q^{-1})/W_d^i(q^{-1})$, $W_n^i(q^{-1})$ is a stable polynomial, and $W_d^i(q^{-1})$ contains the zeros on $|q| \ge 1$ for rejecting the corresponding output disturbance. Moreover, the constraint (18b) gives the following result:

$$C^i(q^{-1})W_n^i(q^{-1})\bar{A}_-^i(q^{-1})\Phi^i(q^{-1}) - \rho^i W_d^i(q^{-1})A_-^i(q^{-1})\bar{\Phi}^i(q^{-1}) = q^{-d^i}B_-^i(q^{-1})Q^i(q^{-1}) \tag{20}$$

where $n_\phi^i = d^i + n_{b_-}^i - 1$ and $n_q^i = n_c^i + n_{w_n}^i + n_{a_-}^i - 1$. Or

$$C^i(z_j^i)W_n^i(z_j^i)\bar{A}_-^i(z_j^i)\Phi^i(z_j^i) - \rho^i W_d^i(z_j^i)A_-^i(z_j^i)\bar{\Phi}^i(z_j^i) = 0. \tag{21}$$

By the solution of ρ^i and $\Phi^i(q^{-1})$ from (21), the following equations are accomplished from (8c) and (19)

$$A_c^i(q^{-1}) = C^i(q^{-1})A_+^i(q^{-1})W_n^i(q^{-1})\bar{A}_-^i(q^{-1})\Phi^i(q^{-1})\tilde{X}^i(q^{-1}) \tag{22}$$

$$R^i(q^{-1}) = \rho^i W_d^i(q^{-1})\bar{\Phi}^i(q^{-1})\tilde{X}^i(q^{-1}). \tag{23}$$

Comparing (22) and (17) gives

$$\begin{aligned}\tilde{X}^i(q^{-1}) &= G_{r+}^i(q^{-1})B_+^i(q^{-1})\hat{X}^i(q^{-1}),\\ X^i(q^{-1}) &= A_+^i(q^{-1})W_n^i(q^{-1})\bar{A}_-^i(q^{-1})\Phi^i(q^{-1})\hat{X}^i(q^{-1})\end{aligned} \tag{24}$$

where $\hat{X}^i(q^{-1})$ is a stable polynomial. Then from (22)-(24)

$$A_c^i(q^{-1}) = C^i(q^{-1})A_+^i(q^{-1})W_n^i(q^{-1})\bar{A}_-^i(q^{-1})\Phi^i(q^{-1})G_{r+}^i(q^{-1})B_+^i(q^{-1})\hat{X}^i(q^{-1}) \tag{25}$$

$$R^i(q^{-1}) = \rho^i W_d^i(q^{-1})\bar{\Phi}^i(q^{-1})G_{r+}^i(q^{-1})B_+^i(q^{-1})\hat{X}^i(q^{-1}). \tag{26}$$

Substituting the relations (25), (26), and (20) into (9) yields

$$S^i(q^{-1}) = G_{r+}^i(q^{-1})A_+^i(q^{-1})Q^i(q^{-1})\hat{X}^i(q^{-1}). \tag{27}$$

From (16) and (24), the $T^i(q^{-1})$ is attained as follows:

$$T^i(q^{-1}) = M^i(q^{-1})A_+^i(q^{-1})W_n^i(q^{-1})\bar{A}_-^i(q^{-1})\Phi^i(q^{-1})\hat{X}^i(q^{-1}). \tag{28}$$

That is, the control polynomials $\{R^i(q^{-1}), S^i(q^{-1}), T^i(q^{-1})\}$ for the dead-beat and the minimax optimization of the output disturbance with respect to the switching surface are achieved from (26)-(28).

3.3 Switching Control for Enhanced Robustness

The proposed switching control is designed as follows:

$$u_{sw}^i(k) = \begin{cases} -A_c^i(q^{-1})\{\sigma^i(k) + \beta^i(q^{-1})v_{sw}^i(k)\}/\{B_+^i(q^{-1})C^i(q^{-1})\bar{B}_-^i(q^{-1})\} \\ \quad \text{if } |\sigma^i(k)| > \chi^i(k) \\ 0, \quad \text{otherwise} \end{cases} \tag{29}$$

where $A_c^i(q^{-1})$ is the same as (25), $\beta^i(q^{-1})$ is a causal stable rational weighting function, $v_{sw}^i(k)$ is given in (38), and $\chi^i(k)$ is described in (39). Substituting (29), (8c) and (9) into (8a) gives

$$\begin{aligned}\sigma^i(k) &= H^i(q^{-1})\delta(k) + \left[W^i(q^{-1})V^i(q^{-1})\right]^* d_o^i(k)\\ &+ B_-^i(q^{-1})\sigma^i(k-d^i)/\bar{B}_-^i(q^{-1}) + \eta^i(q^{-1})v_{sw}^i(k-d^i)\end{aligned} \tag{30}$$

where $\eta^i(q^{-1}) = \beta^i(q^{-1})B_-^i(q^{-1})/\bar{B}_-^i(q^{-1})$. The results of the first and second terms in the left hand side of (30) are obtained from sections 3.1 and 3.2, respectively.

Based on (4), the signal $\left[W^i(q^{-1})V^i(q^{-1})\right]^* d_o^i(k)$ in (30) contains the effect of the switching control of the *ith* subsystem, i.e., $v_{sw}^i(k-d^i)$. From (4b), (6) and (7), the following equation is assume to be true.

$$\begin{aligned}&\left[W^i(q^{-1})V^i(q^{-1})\right]^* d_o^i(k) = \gamma_1^i(k)v_{sw}^i(k-d^i)\\ &+ \textstyle\sum_{j=1}^2 \gamma_{2j}^i(k)\sigma^j(k-d^j) + \gamma_3^i(k)\end{aligned} \tag{31}$$

where $|\gamma_1^i(k)| < \delta_1 < 1, |\gamma_{2j}^i(k)| < \delta_{2j}$, and $|\gamma_3^i(k)| < \delta_3, \forall i, j, k.$

Define the difference of $\sigma^i(k)$ as follows:

$$\Delta\sigma^i(k) = \sigma^i(k+d^i) - \sigma^i(k). \tag{32}$$

Then from (30), (31) and (32)

$$\Delta\sigma^i(k) = \Lambda^i(k) + \left[1 - \tau^i(q^{-1}, k)\right] v_{sw}^i(k) \tag{33}$$

where

$$\tau^i(q^{-1}, k) = 1 - \eta^i(q^{-1}) - \gamma_1^i(k) \tag{34}$$

$$\begin{aligned}\Lambda^i(k) &= H^i(q^{-1})\delta(k+d^i)\\ &+ \left\{\gamma_2^i(k+d^i) + \left[B_-^i(q^{-1}) - \bar{B}_-^i(q^{-1})\right]/\bar{B}_-^i(q^{-1})\right\}\sigma^i(k)\\ &+ \gamma_{2j}^i(k+d^i)\sigma^j(k-d^j+d^i) + \gamma_3^i(k+d^i),\ j \ne i.\end{aligned} \tag{35}$$

The upper bound of $\Lambda^i(k)$ is estimated as follows:

$$|\Lambda^i(k)| \le g_\lambda^i(k) = \lambda_0^i|\sigma^i(k)| + \lambda_1^i|\sigma^j(k)| + \lambda_2^i \tag{36}$$

where $\lambda_1^i \ge 0$, $\left[(1-\lambda^i)^2 - \varepsilon^i(1+\lambda^i)^2\right]/\left[4(1+\lambda^i)\right] > \lambda_0^i \ge 0$, $1 > (1-\lambda^i)^2/(1+\lambda^i)^2 > \varepsilon^i > 0$, and $1 > \lambda^i = \delta_1 + \upsilon^i$, satisfying the following inequality:

$$\left\|1 - \eta^i(q^{-1})\right\|_\infty \le \upsilon^i < 1, \text{ on } D^i \tag{37}$$

where $D^i = \{q \in C \,\|q| < 1\}$ is the domain containing the poles of $\beta^i(q^{-1})$ and the zeros of $\bar{B}_-^i(q^{-1})$. The control in (38) is then employed to deal with the unmodeled dynamics $\Lambda^i(k)$.

$$\begin{cases} v_{sw}^i(k) = -\xi^i(k)g_\lambda^i(k)\sigma^i(k)/\left[(1-\lambda^i)(1+\lambda^i)|\sigma^i(k)|\right], \\ \text{if } |\sigma^i(k)| > \chi^i(k) \\ u_{sw}^i(k) = 0, \quad \text{otherwise} \end{cases} \tag{38}$$

where

$$\begin{aligned}\chi^i(k) = \max\Big\{&4(1+\lambda^i)(\lambda_1^i|\sigma^j(k)| + \lambda_2^i)/\\ &\left[(1-\lambda^i)^2 - \varepsilon^i(1+\lambda^i)^2 - 4(1+\lambda^i)\lambda_0^i\right],\\ &4(1+\lambda^i)g_\lambda^i(k)/\left[(1-\lambda^i)^2 - \varepsilon^i(1+\lambda^i)^2\right]\Big\},\ j \ne i.\end{aligned} \tag{39}$$

The switching gain satisfies the following inequality:

$$\xi_2^i(k) > \xi^i(k) > \xi_1^i(k) \ge 0 \tag{40}$$

where

$$\xi_{1,2}^i(k) = g_1^i(k) \mp \sqrt{\left[g_1^i(k)\right]^2 - g_2^i(k)} \tag{41}$$

$$g_1^i(k) = (1-\lambda^i)^2|\sigma^i(k)|/[(1+\lambda^i)g_\lambda^i(k)] - (1-\lambda^i) \tag{42}$$

$$g_2^i(k) = (1-\lambda^i)^2\left\{\left[g_\lambda^i(k)\right]^2 + 2g_\lambda^i(k)|\sigma^i(k)| + \varepsilon^i|\sigma^i(k)|^2\right\}/\left[g_\lambda^i(k)\right]^2. \tag{43}$$

Theorem 1: Consider the system (4) and the controller (6) with $u_{sw}^i(k)$ in (29) and $v_{sw}^i(k)$ in (38). The polynomials $R^i(q^{-1}), S^i(q^{-1})$ and $T^i(q^{-1})$ are achieved from (26)-(28). The inequalities in (36) and (37) are satisfied. Then $\{u^i(k)\}$ is bounded, $\{\sigma^i(k)\}$ is bounded in the sense of the minimal weighted sensitivity between switching surface and output disturbance, and the following performance (44) is accomplished.

$$D_\sigma = \left\{\sigma^i(k) : \left|\sigma^i(k)\right| \le \chi^i(k)\right\}. \tag{44}$$

Proof: See [5] for a similar result.

IV. EXPERIMENTS

4.1 Experimental Setup

The first and second links are individually driven by the same permanent magnet DC motor. The length and mass of the first and second links are 83mm, 0.826kg and 103mm, 0.214kg, respectively. The DC motor, gear box, and driver are A-max32 motor, Gp32C, and 4-Q-DC servo control LSC30/2 of Maxon, respectively. The DSP-chip of TMS320F240 is to realize the DCRD. A 12bits DA converter is used to send the control signal; a quadrature encoder/counter interface is applied to feedback the position of the motor to the DSP chip. To communicate these interfaces with DSP chip, a CPLD is employed to select the signal from the address bus of the DSP chip.

4.2 Control Performance

In this study, $T_s = 8ms$, $\sigma^i(k) = e^i(k) - 0.5e^i(k-1) + 0.2e^i(k-2)$, $\beta^i(q^{-1}) = (1.5 - 0.3q^{-1})/(1.4 - 0.4q^{-1})$, $\lambda_0^i = \lambda_1^i = 0.001$, $\lambda_2^i = \bar{\lambda}^i = 0.01$, $\varepsilon^i = 0.4$, and $\xi^i(k) = \xi_1^i(k) + 0.3g_1^i(k)\left\{1 - 0.99e^{-1000\left|\sigma^i(k)\right|}\right\}$ are set.

The response of the system without payload for $r^i(t) = 30°(1 - \cos(0.6\pi t)), i = 1,2$ is shown in Fig. 4. The corresponding e_{ssm} is also shown in Table 1. Similarly, the Fig. 4 case without switching control is shown in Fig. 5. The performance is still acceptable. The output responses for the other reference inputs are also acceptable; for simplicity, only the corresponding e_{ssm} is shown in Table 1. For authenticating the effectiveness of the proposed control, the Fig. 4 case with 3.28 kg payload fastened on the bottom of the second link is studied; the related result is then presented in Fig. 6 that is satisfactory (see Table 1). On the contrary, the output response of Fig. 6 by the proportional control is poorer than that of Fig. 6 (see Table 1). For simplicity, only the output response by the proportional control for $r^i(t) = 30°(1 - \cos(0.4\pi t)), i = 1,2$ is shown in Fig. 7. Finally, the response of Fig. 6 case by $W^i(q^{-1}) = \hat{W}(q^{-1}) = 1/\left[(1 - q^{-1})(1 - 2\cos(wh)q^{-1} + q^{-2})\right]$, where $i=1,2$ $w = 100\pi$ (rad), is shown in Fig. 8. Indeed, the weighted function can tackle the payload to obtain a better tracking result; however, some high-frequency components of the control input occur (see Figs. 8(g) and (h)). Because the system is subjected to the uncertainties, the operating point is in the neighborhood of the switching surface (see Figs. 8 (e) and (f)). The other output responses of the system with 3.28 kg payload are also satisfactory. For brevity, only the related e_{ssm} are shown in Table 1.

From the above analysis, the advantages of the DCRD are summarized as follows:

(i) The DCRD for the legged robot is simple because the system identification and the controller design of every link are individually obtained.

(ii) A suitable selection of weighted function, e.g., $W^i(q^{-1}) = \hat{W}(q^{-1}), i = 1,2,$ influences the system performance much. However, the switching control can further enhance the system performance.

(iii) It is effective because the on-line identification is not required and the system performance is excellent.

V. CONCLUSION

In this paper, the trajectory tracking of a two-degree-of-freedom legged robot using TMSC320F240-based decentralized control with robust designs is developed. Each link is modeled by a second-order linear discrete-time system. The output disturbance of every link includes interaction stemming from the other link, external load, and modeling error. It is huge and contains various frequencies. The H^∞-norm of the weighted sensitivity function between the switching surface and output disturbance is then minimized to attenuate its effect. An appropriate weighting function to reject the related output disturbance is much more important than the role of a switching control. However, the switching control does not need the information of the output disturbance and can further improve the system performance. The system identification and controller design only for each link are required. The experiments of the legged robot with 3.28kg payload that is much larger than that of the DC motor (i.e., 0.5 kg) confirm the validity of the proposed control scheme.

Acknowledgement: The authors would like to thank the financial support form Tatung University with Grant No. B91-M07-035 and the National Science Council of R.O.C. with Grant No. NSC91-2212-E-036-006.

REFERENCES

[1] X. Chen, K. Watanabe, K. Kiguchi and K. Izumi, "An ART-based fuzzy controller for the adaptive navigation of a quadruped robot," *IEEE/ASME Trans. Mechatron.*, vol. 7, no. 3, pp. 318-328, 2002.

[2] D. D. Sijak, *Large-Scale Dynamic Systems: Stability and Structure.* North-Holland, 1978.

[3] K.J. Astrom and B. Wittenmark, Computer-Controlled Systems-- Theory and Design, Prentice-Hall Inc., 3rd Ed., 1997.

[4] K. D. Young, V. I. Utkin and Ümit Özgüner, "A control Engineer's guide to sliding mode control," *IEEE Trans. Contr. Syst. Technol.*, vol. 7, no. 3, pp. 328-342, 1999.

[5] C. L. Hwang, "Robust discrete variable structure control with finite-time approach to switching surface," *IFAC, Int. J. of Automatica,* vol. 38, no. 1, pp. 167-175, 2002.

[6] C. L. Hwang and C. Jan, "Optimal and reinforced robustness designs of fuzzy variable structure tracking control for a piezoelectric actuator system," IEEE

Trans. Fuzzy Syst., vol. 11, no. 4, pp. 507-517, 2003.
[7] C. L. Hwang and B. S. Chen, "Adaptive control of optimal model matching in H^{∞}-norm space," IEE Proc. D, Contr. Theory, Applicat., vol. 135, no. 4, 295-301, 1988.

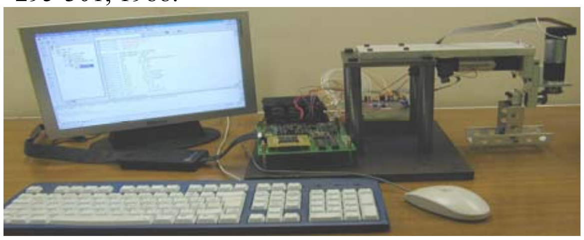

Fig. 1. Experimental setup of legged robotic system.

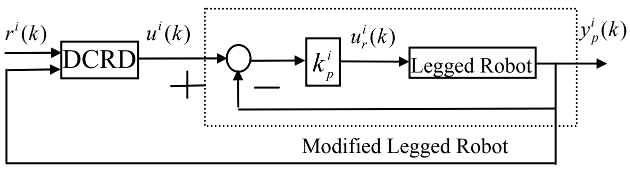

Fig. 2. Control block diagram of the *ith* subsystem.

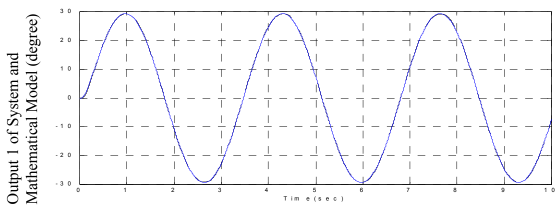

(a) $f^1 = 0.3Hz, u_m^1 = 30^{\circ}$.

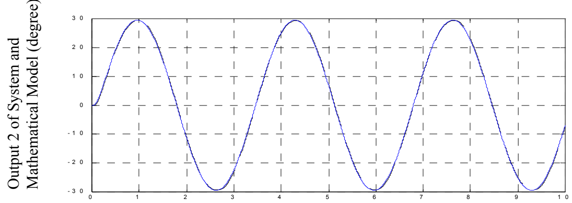

(b) $f^2 = 0.3Hz, u_m^2 = 30^{\circ}$.

Fig. 3. The output responses of the mathematical model $(-)$ and the system $(\cdots)$ for the input $u^i(t) = u_m^i \sin(2\pi f^i t), i = 1,2$.

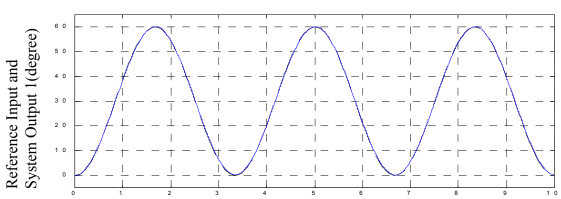

(a) $r^1(t)(\cdots), y^1(t)(-)$.

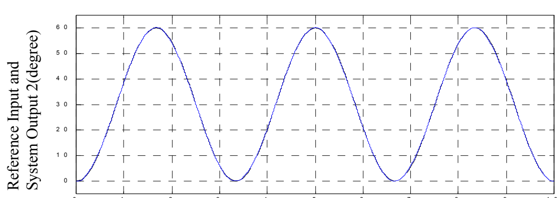

(b) $r^2(t)(\cdots), y^2(t)(-)$.

Fig. 4. The response of the system without payload by using the proposed control with $W^i(q^{-1}) = 1$ for $r^i(t) = 30^{\circ}(1 - \cos(0.6\pi t)), i = 1,2$.

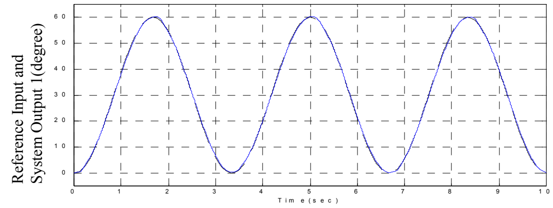

(a) $r^1(t)(\cdots), y^1(t)(-)$.

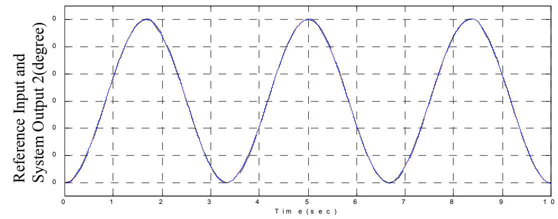

(b) $r^2(t)(\cdots), y^2(t)(-)$.

Fig. 5. The output response of Fig. 4 for the proposed control without switching control.

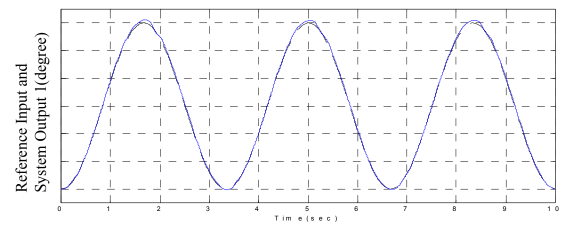

(a) $r^1(t)(\cdots), y^1(t)(-)$.

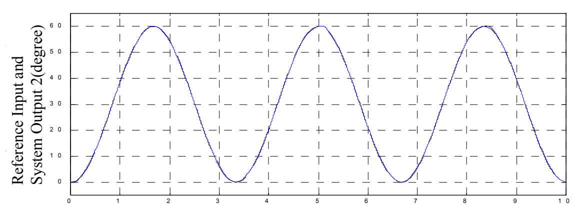

(b) $r^2(t)(\cdots), y^2(t)(-)$.

Fig. 6. The output response of Fig. 4 with 3.28*kg* payload

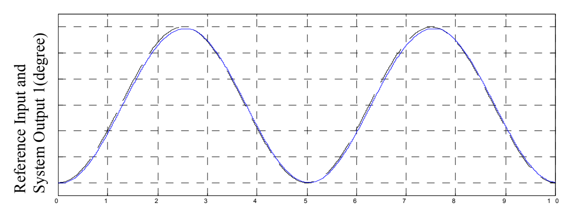

(a) $r^1(t)(\cdots), y^1(t)(-)$.

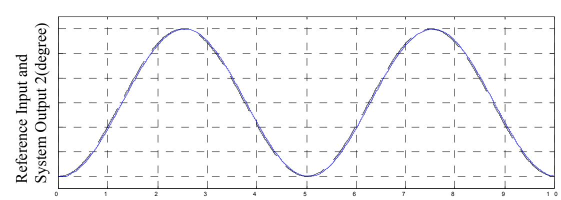

(b) $r^2(t)(\cdots), y^2(t)(-)$.

Fig. 7. The output response of the system with 3.28*kg* payload for $r^i(t) = 30^{\circ}(1 - \cos(0.4\pi t)), i = 1,2$ by the proportional control with $K_p = diag\{120 \quad 120\}$.

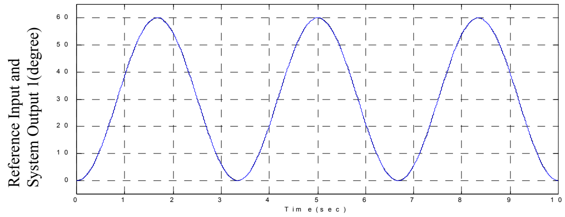

(a) $r^1(t)(\cdots), y^1(t)(-)$.

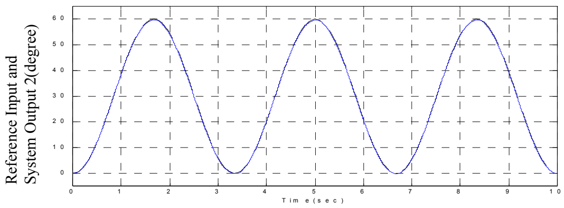

(b) $r^2(t)(\cdots), y^2(t)(-)$.

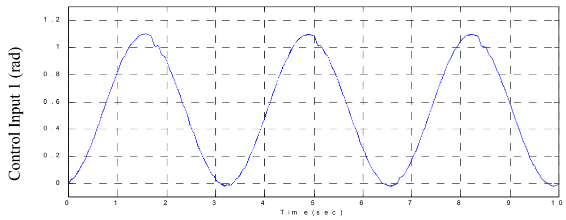

(c) $u^1(t)$.

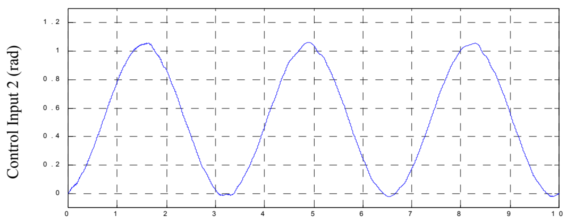

(d) $u^2(t)$.

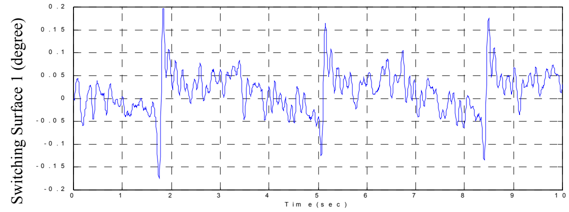

(e) $\sigma^1(t)$.

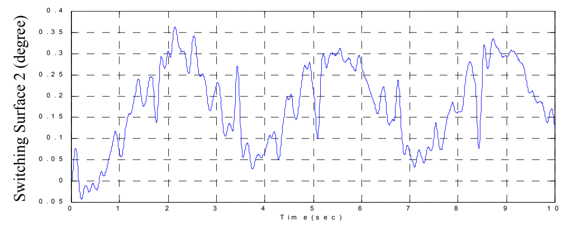

(f) $\sigma^2(t)$.

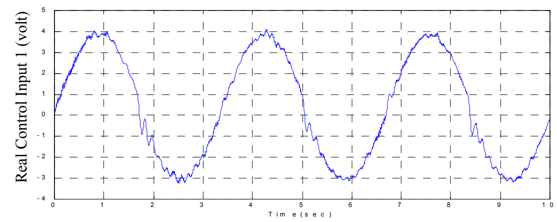

(g) $u_r^1(t)$.

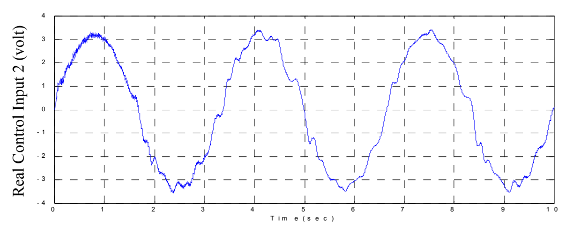

(h) $u_r^2(t)$.

Fig. 8. The response of the system with 3.28 *kg* payload by the proposed control with $W^i(q^{-1}) = \hat{W}(q^{-1})$ for $r^i(t) = 30°(1-\cos(0.6\pi t)), i = 1,2$.

Table 1. The maximum steady-state tracking error (degree and % relative to the corresponding amplitude of the reference input) for various controls and reference inputs: $r^i(k) = r_m^i\left[1-\cos(2\pi f^i kT_s)\right], i = 1,2$.

Payload	No					3.28 *kg*				
Weighting	-	$W^i(q^{-1})=1$		$W^i(q^{-1})=\hat{W}(q^{-1})$		-	$W^i(q^{-1})=1$		$W^i(q^{-1})=\hat{W}(q^{-1})$	
Case \ Control	P Control ($k_p^i = 120$)	Equivalent Control	DCRD	Equivalent Control	DCRD	P Control ($k_p^i = 120$)	Equivalent Control	DCRD	Equivalent Control	DCRD
$f^1 = 0.2Hz, r_m^1 = 30°$	2.30(3.82%)	2.01(3.34%)	1.52(2.54%)	0.51(0.85%)	0.47(0.78%)	2.38(3.97%)	7.62(12.69%)	2.07(3.45%)	0.94(1.57%)	0.60(1.00%)
$f^2 = 0.2Hz, r_m^2 = 30°$	2.20(3.68%)	2.13(3.54%)	1.65(2.75%)	0.44(0.73%)	0.39(0.65%)	2.31(3.84%)	2.82(4.71%)	1.43(2.38%)	0.99(1.65%)	0.52(0.87%)
$f^1 = 0.3Hz, r_m^1 = 30°$	3.30(5.50%)	1.50(2.50%)	0.99(1.65%)	0.50(0.83%)	0.41(0.68%)	2.37(3.95%)	6.46(10.76%)	2.19(3.65%)	0.88(1.47%)	0.54(0.90%)
$f^2 = 0.3Hz, r_m^2 = 30°$	3.19(5.32%)	1.59(2.65%)	0.89(1.49%)	0.57(0.95%)	0.48(0.79%)	2.36(3.93%)	2.61(4.36%)	1.49(2.49%)	0.74(1.24%)	0.55(0.92%)
$f^1 = 0.4Hz, r_m^1 = 30°$	4.33(7.22%)	2.50(4.18%)	1.59(2.66%)	0.57(0.95%)	0.59(0.98%)	4.31(7.19%)	4.94(8.23%)	2.32(3.87%)	1.08(1.81%)	0.95(1.58%)
$f^2 = 0.4Hz, r_m^2 = 30°$	4.15(6.92%)	1.87(3.12%)	1.22(2.03%)	0.44(0.74%)	0.41(0.69%)	4.33(7.21%)	2.14(3.57%)	1.98(3.30%)	0.79(1.32%)	0.54(0.91%)